JOURNAL OF THEORETICAL AND APPLIED MECHANICS
60, 2, pp. 279-292, Warsaw 2022
https://doi.org/10.15632/jtam-pl/149175

FREE VIBRATION ANALYSIS OF FGM STEPPED NANOSTRUCTURES USING NONLOCAL DYNAMIC STIFFNESS MODEL

Tran Van Lien
Hanoi University of Civil Engineering, Vietnam
e-mail: LienTV@huce.edu.vn
Ngo Trong Duc
Fujita Corporation, Vietnam
Tran Binh Dinh
Hanoi University of Civil Engineering, Vietnam
Pham Tuan Dat
Le Quy Don Technical University, Vietnam

A nonlocal Dynamic Stiffness Model (DSM) for free vibration analysis of Functionally Graded Material (FGM) stepped nanostructures based on the Nonlocal Elastic Theory (NET) is proposed. An exact solution to the equation of motion of a nanobeam element according to the Timoshenko beam theory, NET, and taking into account position of the neutral axis is constructed. Nondimensional frequencies and mode shapes of complete FGM stepped nanostructures are easily obtained using the nonlocal DSM. Numerical results are presented to show significance of the material distribution profile, nonlocal effect, and boundary conditions on free vibration of nanostructures.

Keywords: nonlocal, DSM, FGM, nanostructure, nondimensional frequency

1. Introduction

Functionally Graded Materials (FGMs) are a new generation composite materials that are made up of two or more component materials with a continuous variation in the ratio of the components in one or more directions. FGMs are employed in micro/nano electro-mechanical systems (MEMS/NEMS) to archive high sensitivity and desired performance. Nano-sized structures such as plates, sheets, beams and framed structures are widely used in NEMS devices. Steps in nanostructures are considered as abrupt changes in the cross-sectional area such as CNT heterojunctions or two connected nanobeam portions with different material properties. Steps in nanostructures may be manufactured on the purpose of attaining desired frequencies in some applications such as a piezoelectric energy harvester (Usharani *et al.*, 2018) or building blocks of nanoelectromechanical and micro-electromechanical systems. However, steps in structures may occur as a manufacturing defect. For this reason, stepped nanostructures are especially attracting more and more attention due to their various potential applications.

Because of the size effect, classical elasticity theory cannot fully and accurately investigate the mechanical behaviour of nanostructures. Therefore, Nonlocal Elasticity Theory (NET) was first proposed by Eringen (2002) assuming that the stress tensor at one point is not only a function of deformation but also includes all surrounding ones. Currently, NET is widely used to formulate differential equations of motion of nanostructures using homogeneous materials and FG materials. Reddy (2007) established equations of vibration and stability of homogeneous nanobeams according to the NET for Euler-Bernoulli, Timoshenko, Reddy and Levinson beam

theories. Many other authors have developed analytical methods (Wang *et al.*, 2007), Rayleight--Ritz method (Chakraverty and Behera, 2015), Finite Element Method (FEM) (Eltaher *et al.*, 2013b), differential transform method (Ebrahimi and Nasirzadeh, 2015), differential quadrature method (Jena and Chakraverty, 2018), and so on to consider bending, stability and free vibration problems of nanobeams from homogeneous materials.

Şimşek and Yurtcu (2013), Rahmani and Pedram (2014) simultaneously studied bending and buckling of Timoshenko FGM nanobeams using analytical methods. In addition, Mechab *et al.* (2016) studied free vibration, while Uymaz (2013) researched on forced vibration of nanobeams, both using higher-order shear deformation theory. Ebrahimi and Salari (2015) exploited a semi--analytical method to study vibration and buckling of Euler-Bernoulli FGM nanobeams considering position of the physical neutral axis. Malikan *et al.* (2021) applied the Galerkin weighted residual method to address the axial stability and bifurcation point of a functionally graded piezomagnetic structure containing flexomagneticity in a thermal environment. A spectral finite element formulation was indicated by Narendar and Gopalakrishnan (2011) to investigate vibration of nonlocal continuum beams. The analytical solutions found above are all in Navier's series, thus, they are limited to simply supported beams. For other boundary conditions, the authors applied the FEM to analyze free vibration and buckling of FGM nanobeams according to Euler-Bernoulli beam theory (Eltaher *et al.*, 2013a) and Timoshenko theory (Aria and Friswell, 2019). Recently, the authors of (Trinh *et al.*, 2018) found the solution for natural frequencies and mode shapes of microbeams under various boundary conditions using the state-space concepts.

As the FEM is formulated on the base of a frequency-independent polynomial shape function, it could not be used to capture all necessary high frequencies and mode shapes of interest. An alternative approach called the Dynamic Stiffness Model (DSM) fulfilled the gap of the FEM by using frequency-dependent shape functions that are considered as an exact solution of the vibration problem in the frequency domain (Su and Banerjee, 2015; Lien *et al.*, 2019). Although exact solutions of the vibration problem are not easily constructed for complete structures, but they, if available, are enable to study the exact response of the structure in an arbitrary frequency range. Karličić *et al.* (2015) obtained the dynamic stiffness matrix of a nonlocal homogenous rod in the closed form. The frequency response function obtained using the proposed DSM shows extremely high modal density near the maximum frequency. Recently, Taima *et al.* (2020) studied free vibration of multi-stepped Bernoulli-Euler nanobeams made of homogenous materials using DSM.

To the best of the authors' knowledge, the DSM based approach to nonlocal FGM nanostructures presents a gap that has to be fulfilled. In the present work, a nonlocal DSM is developed to investigate free vibration characteristics of FGM stepped nanostructures on the basis of NET and Timoshenko beam theory. Comparison between the obtained and published results shows the reliability of the method. The effect of the nonlocal, material distribution profile and geometry parameters on the vibration frequency and mode shapes of nanostructures with different boundary conditions has been studied in detail.

2. Nonlocal DSM of a FGM nanostructure

For an FGM nanobeam (Fig. 1), the material properties vary along the thickness direction, and are assumed to take the form (Eltaher *et al.*, 2013a)

$$P(z) = P_b + (P_t - P_b)\Big(\frac{z}{h} + \frac{1}{2}\Big)^{\kappa} \qquad -\frac{1}{2}h \leqslant z \leqslant \frac{1}{2}h \tag{2.1}$$

where P stands for Young's modulus E, shear modulus G and mass density ρ, respectively, the subscripts t and b refer to the corresponding values of the top and bottom layer materials,

κ is the volume fraction index, and z is the coordinate from the mid-plane of the beam. The displacement field of the Timoshenko beam is given by

$$u(x,z,t) = u_0(x,t) - (z-h_0)\theta(x,t) \qquad w(x,z,t) = w_0(x,t) \tag{2.2}$$

where $u_0(x,t)$, $w_0(x,t)$ are the axial displacement, deflection of a point on the neutral axis, respectively, h_0 is the distance from the neutral axis to x-axis, θ is the angle of rotation of the cross-section around the y-axis. From there, we get the strain components

$$\varepsilon_{xx} = \frac{\partial u_0}{\partial x} - (z-h_0)\frac{\partial \theta}{\partial x} \qquad \gamma_{xz} = \frac{\partial w_0}{\partial x} - \theta = -\varphi \tag{2.3}$$

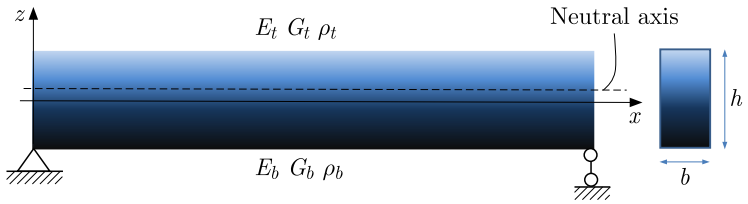

Fig. 1. An FGM nanobeam

The nonlocal constitute equations for nanobeams can be written in the form (Eringen, 2002)

$$\sigma_{xx} - \mu\frac{\partial^2 \sigma_{xx}}{\partial x^2} = E\varepsilon_{xx} \qquad \sigma_{xz} - \mu\frac{\partial^2 \sigma_{xz}}{\partial x^2} = G\gamma_{xz} \tag{2.4}$$

where $\mu = e_0^2 a^2$ is a nonlocal parameter, e_0 is a constant associated with each material, a is the internal characteristic length. Using the Hamilton principle, equations of free vibration for the FGM nanobeam can be derived in the form

$$\begin{aligned}
&A_{11}\frac{\partial^2 u_0}{\partial x^2} - A_{12}\frac{\partial^2 \theta}{\partial x^2} - I_{11}\frac{\partial^2 u_0}{\partial t^2} + I_{12}\frac{\partial^2 \theta}{\partial t^2} + \mu\Big(I_{11}\frac{\partial^4 u_0}{\partial x^2 \partial t^2} - I_{12}\frac{\partial^4 \theta}{\partial x^2 \partial t^2}\Big) = 0\\
&A_{22}\frac{\partial^2 \theta}{\partial x^2} - A_{12}\frac{\partial^2 u_0}{\partial x^2} + A_{33}\Big(\frac{\partial w_0}{\partial x} - \theta\Big) - I_{22}\frac{\partial^2 \theta}{\partial t^2} + I_{12}\frac{\partial^2 u_0}{\partial t^2} - \mu I_{12}\frac{\partial^4 u_0}{\partial x^2 \partial t^2}\\
&\quad + \mu I_{22}\frac{\partial^4 \theta}{\partial x^2 \partial t^2} = 0\\
&A_{33}\Big(\frac{\partial^2 w_0}{\partial x^2} - \frac{\partial \theta}{\partial x}\Big) - I_{11}\frac{\partial^2 w_0}{\partial t^2} + \mu I_{11}\frac{\partial^4 w_0}{\partial x^2 \partial t^2} = 0
\end{aligned} \tag{2.5}$$

and the corresponding boundary conditions

$$\begin{aligned}
&u_0 = 0 \quad \text{or} \quad A_{11}\frac{\partial u_0}{\partial x} - A_{12}\frac{\partial \theta}{\partial x} + \mu\Big(I_{11}\frac{\partial^3 u_0}{\partial x \partial t^2} - I_{12}\frac{\partial^3 \theta}{\partial x \partial t^2}\Big) = 0\\
&w_0 = 0 \quad \text{or} \quad A_{33}\Big(\frac{\partial w_0}{\partial x} - \theta\Big) + \mu I_{11}\frac{\partial^3 w_0}{\partial x \partial t^2} = 0\\
&\theta_0 = 0 \quad \text{or} \quad A_{12}\frac{\partial u_0}{\partial x} - A_{22}\frac{\partial \theta}{\partial x} + \mu\Big(I_{11}\frac{\partial^2 w_0}{\partial t^2} + I_{12}\frac{\partial^3 u_0}{\partial x \partial t^2} - I_{22}\frac{\partial^3 \theta}{\partial x \partial t^2}\Big) = 0
\end{aligned} \tag{2.6}$$

where A_{11}, A_{12}, A_{22} and A_{33} are the rigidities, and I_{11}, I_{12} and I_{22} are the mass moments of inertia

$$\begin{aligned}
&(A_{11}, A_{12}, A_{22}) = \int_A E(z)\left(1, z-h_0, (z-h_0)^2\right)\, dA \qquad A_{33} = \eta\int_A G(z)\, dA\\
&(I_{11}, I_{12}, I_{22}) = \int_A \rho(z)\left(1, z-h_0, (z-h_0)^2\right)\, dA
\end{aligned} \tag{2.7}$$

where η is the shear correction factor, $\eta = 5/6$ for a rectangular cross-section. Neglecting the influence of the axial displacement and the nonlocality effect, the position of the neutral axis h_0 can be written by (Eltaher *et al.*, 2013a)

$$h_0 = \frac{\kappa(R_E - 1)h}{2(\kappa + 2)(\kappa + R_E)} \qquad R_E = \frac{E_t}{E_b} \tag{2.8}$$

Setting

$$[U, \Theta, W] = \int_{-\infty}^{\infty} [u_0(x,t), \theta(x,t), w_0(x,t)]\mathrm{e}^{-\mathrm{i}\omega t}\, dt \tag{2.9}$$

Equations of vibration (2.5) in the frequency domain can be obtained as

$$\begin{aligned}
&(A_{11} - \mu I_{11}\omega^2)\frac{d^2U}{dx^2} - (A_{12} - \mu I_{12}\omega^2)\frac{d^2\Theta}{dx^2} + I_{11}\omega^2 U - I_{12}\omega^2\Theta = 0\\
&-(A_{12} - \mu I_{12}\omega^2)\frac{d^2U}{dx^2} + (A_{22} - \mu I_{22}\omega^2)\frac{d^2\Theta}{dx^2} + A_{33}\frac{dW}{dx} - I_{12}\omega^2 U\\
&\quad + (I_{22}\omega^2 - A_{33})\Theta = 0\\
&(A_{33} - \mu I_{11}\omega^2)\frac{d^2W}{dx^2} - A_{33}\frac{d\Theta}{dx} + I_{11}\omega^2 W = 0
\end{aligned} \tag{2.10}$$

Putting into the matrices and vectors as follows

$$\begin{aligned}
&\widetilde{\mathbf{A}} = \begin{bmatrix} A_{11} - \mu I_{11}\omega^2 & -(A_{12} - \mu I_{12}\omega^2) & 0\\ -(A_{12} - \mu I_{12}\omega^2) & A_{22} - \mu I_{22}\omega^2 & 0\\ 0 & 0 & A_{33} - \mu I_{11}\omega^2 \end{bmatrix} \qquad \mathbf{z} = \begin{bmatrix} U\\ \Theta\\ W \end{bmatrix}\\
&\widetilde{\mathbf{B}} = \begin{bmatrix} 0 & 0 & 0\\ 0 & 0 & A_{33}\\ 0 & -A_{33} & 0 \end{bmatrix} \qquad \widetilde{\mathbf{C}} = \begin{bmatrix} I_{11}\omega^2 & -I_{12}\omega^2 & 0\\ -I_{12}\omega^2 & I_{22}\omega^2 - A_{33} & 0\\ 0 & 0 & I_{11}\omega^2 \end{bmatrix}
\end{aligned} \tag{2.11}$$

equations (2.10) can now be described in the form of

$$\widetilde{\mathbf{A}}\mathbf{z}'' + \widetilde{\mathbf{B}}\mathbf{z}' + \widetilde{\mathbf{C}}\mathbf{z} = \mathbf{0} \tag{2.12}$$

Choosing solutions to Eq. (2.12) in the form of $\mathbf{z}_0 = \mathbf{d}\exp(\lambda x)$ leads to

$$(\lambda^2\widetilde{\mathbf{A}} + \lambda\widetilde{\mathbf{B}} + \widetilde{\mathbf{C}})\mathbf{d} = \mathbf{0} \tag{2.13}$$

Equation (2.13) have non-trivial solutions when

$$\det(\lambda^2\widetilde{\mathbf{A}} + \lambda\widetilde{\mathbf{B}} + \widetilde{\mathbf{C}}) = 0 \tag{2.14}$$

We receive cubic equations of $\eta = \lambda^2$: $\eta^3 + a\eta^2 + b\eta + c = 0$. Using notations η_1, η_2, η_3 as solutions to the cubic equations and

$$\lambda_{1,4} = \pm k_1 \qquad \lambda_{2,5} = \pm k_2 \qquad \lambda_{3,6} = \pm k_3 \qquad k_j = \sqrt{\eta_j} \qquad j = 1, 2, 3 \tag{2.15}$$

the general solutions of Eq. (2.12) are in the form as $\mathbf{z}(x,\omega) = \sum_{j=1}^{6}\mathbf{d}_j\exp(\lambda_j x)$. From the first and third equations of (2.12), we yield

$$\mathbf{z}(x,\omega)=\begin{bmatrix}\alpha_1C_1 & \alpha_2C_2 & \alpha_3C_3 & \alpha_4C_4 & \alpha_5C_5 & \alpha_6C_6\\ C_1 & C_2 & C_3 & C_4 & C_5 & C_6\\ \beta_1C_1 & \beta_2C_2 & \beta_3C_3 & \beta_4C_4 & \beta_5C_5 & \beta_6C_6\end{bmatrix}\left[\mathrm{e}^{k_1x},\mathrm{e}^{k_2x},\mathrm{e}^{k_3x},\mathrm{e}^{-k_1x},\mathrm{e}^{-k_2x},\mathrm{e}^{-k_3x}\right]^{\mathrm{T}} \tag{2.16}$$

where $\mathbf{C}=[C_1,\ldots,C_6]^{\mathrm{T}}$ are independent constants and

$$\alpha_1=\frac{(A_{12}-\mu I_{12}\omega^2)k_1^2+I_{12}\omega^2}{(A_{11}-\mu I_{11}\omega^2)k_1^2+I_{11}\omega^2}=\alpha_4 \qquad \beta_1=\frac{A_{33}k_1}{(A_{33}-\mu I_{11}\omega^2)k_1^2+I_{11}\omega^2}=-\beta_4 \tag{2.17}$$

Similarly, $\alpha_2=\alpha_5$, $\beta_2=-\beta_5$, $\alpha_3=\alpha_6$, $\beta_3=-\beta_6$, Eq. (2.16) can be rewritten in the form

$$[\mathbf{z}(x,\omega)]^{\mathrm{T}}=\mathbf{G}(x,\omega)\mathbf{C} \tag{2.18}$$

where

$$\mathbf{G}(x,\omega)=\begin{bmatrix}\alpha_1\mathrm{e}^{k_1x} & \alpha_2\mathrm{e}^{k_2x} & \alpha_3\mathrm{e}^{k_3x} & \alpha_1\mathrm{e}^{-k_1x} & \alpha_2\mathrm{e}^{-k_2x} & \alpha_3\mathrm{e}^{-k_3x}\\ \mathrm{e}^{k_1x} & \mathrm{e}^{k_2x} & \mathrm{e}^{k_3x} & \mathrm{e}^{-k_1x} & \mathrm{e}^{-k_2x} & \mathrm{e}^{-k_3x}\\ \beta_1\mathrm{e}^{k_1x} & \beta_2\mathrm{e}^{k_2x} & \beta_3\mathrm{e}^{k_3x} & -\beta_1\mathrm{e}^{-k_1x} & -\beta_2\mathrm{e}^{-k_2x} & -\beta_3\mathrm{e}^{-k_3x}\end{bmatrix} \tag{2.19}$$

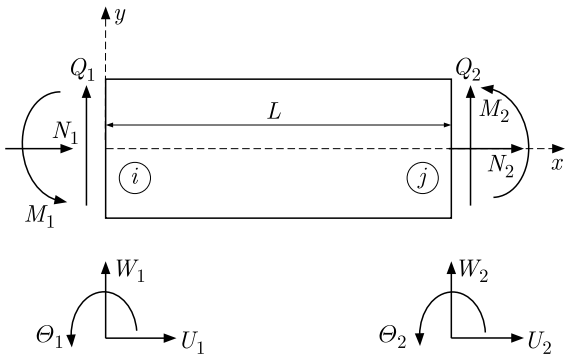

Fig. 2. Node coordinates, nodal loads of a nanobeam element

Let us consider a two-dimensional FGM nanobeam element as shown in Fig. 2. Nodal displacements and forces of the element are introduced as

$$\widehat{\mathbf{U}}_e=[U_1,\Theta_1,W_1,U_2,\Theta_2,W_2]^{\mathrm{T}} \qquad \mathbf{P}_e=[N_1,M_1,Q_1,N_2,M_2,Q_2]^{\mathrm{T}} \tag{2.20}$$

where

$$\begin{aligned}
&U_1=z_1(0,\omega) \qquad \Theta_1=z_2(0,\omega) \qquad W_1=z_3(0,\omega)\\
&U_2=z_1(L,\omega) \qquad \Theta_2=z_2(L,\omega) \qquad W_2=z_3(L,\omega)\\
&N_1=-[(A_{11}-\mu I_{11}\omega^2)\partial_x z_1-(A_{12}-\mu I_{12}\omega^2)\partial_x z_2]_{x=0}\\
&Q_1=-[(A_{33}-\mu I_{11}\omega^2)\partial_x z_3-A_{33}z_2]_{x=0}\\
&M_1=-[(A_{12}-\mu I_{12}\omega^2)\partial_x z_1-(A_{22}-\mu I_{22}\omega^2)\partial_x z_2-\mu I_{11}\omega^2 z_3]_{x=0}\\
&N_2=[(A_{11}-\mu I_{11}\omega^2)\partial_x z_1-(A_{12}-\mu I_{12}\omega^2)\partial_x z_2]_{x=L}\\
&Q_2=[(A_{33}-\mu I_{11}\omega^2)\partial_x z_3-A_{33}z_2]_{x=L}\\
&M_2=[(A_{12}-\mu I_{12}\omega^2)\partial_x z_1-(A_{22}-\mu I_{22}\omega^2)\partial_x z_2-\mu I_{11}\omega^2 z_3]_{x=L}
\end{aligned} \tag{2.21}$$

Substituting expression (2.18) into (2.21), we get

$$\widehat{\mathbf{U}}_e=\begin{bmatrix}\mathbf{G}(0,\omega)\\ \mathbf{G}(L,\omega)\end{bmatrix}\mathbf{C} \qquad \mathbf{P}_e=\begin{bmatrix}-\mathbf{B}_F(\mathbf{G})_{\mathbf{x=0}}\\ \mathbf{B}_F(\mathbf{G})_{x=L}\end{bmatrix}\mathbf{C} \tag{2.22}$$

with $\mathbf{B}_F$ being the matrix operator

$$\mathbf{B}_F = \begin{bmatrix} (A_{11} - \mu I_{11}\omega^2)\partial_x & -(A_{12} - \mu I_{12}\omega^2)\partial_x & 0 \\ (A_{12} - \mu I_{12}\omega^2)\partial_x & -(A_{22} - \mu I_{22}\omega^2)\partial_x & -\mu_{11}\omega^2 \\ 0 & -A_{33} & (A_{33} - \mu I_{11}\omega^2)\partial_x \end{bmatrix} \tag{2.23}$$

Eliminating the constant vector $\mathbf{C}$ in equation (2.22) leads to

$$\mathbf{P}_e(\omega) = \begin{bmatrix} -\mathbf{B}_F(\mathbf{G})_{x=0} \\ \mathbf{B}_F(\mathbf{G})_{x=L} \end{bmatrix} \begin{bmatrix} \mathbf{G}(0,\omega) \\ \mathbf{G}(L,\omega) \end{bmatrix}^{-1} \widehat{\mathbf{U}}_e = \widehat{\mathbf{K}}_e(\omega)\widehat{\mathbf{U}}_e \tag{2.24}$$

where $\widehat{\mathbf{K}}_e$ is the dynamic stiffness matrix of the FGM nanobeam element.

For a given structure that consists of a number of FGM nanobeam elements like above, by means of balancing all the internal forces at every node of the structure, there will be obtained the total dynamic stiffness matrix $\widehat{\mathbf{K}}(\omega)$. Letting $\widehat{\mathbf{U}}$ be the total DOF vector of the structure, the equation of motion for the dynamic stiffness model is

$$\widehat{\mathbf{K}}(\omega)\widehat{\mathbf{U}} = \mathbf{0} \tag{2.25}$$

Therefore, the natural frequencies $\boldsymbol{\omega} = [\omega_1, \omega_2, \ldots, \omega_n]$ can be found from the following equation

$$\det \widehat{\mathbf{K}}(\omega) = 0 \tag{2.26}$$

and the mode shape related to the frequency ω_j is

$$\{\varphi_j(x)\} = C_j^0 \widehat{\mathbf{G}}(x,\omega_j)\widehat{\mathbf{U}}_j \tag{2.27}$$

where

$$\widehat{\mathbf{G}}(x,\omega) = \mathbf{G}(x,\omega) \begin{bmatrix} \mathbf{G}(0,\omega) \\ \mathbf{G}(L,\omega) \end{bmatrix}^{-1} \tag{2.28}$$

C_j^0 is an arbitrary constant and $\widehat{\mathbf{U}}_j$ is the normalized solution corresponding to ω_j.

3. Numerical results and discussion

3.1. Comparison of calculation results and published results

In this Subsection, the numerical results are compared with the published results to validate the present study. The first comparison is made for nondimensional fundamental frequencies $\lambda_1 = \omega_1 L^2/\sqrt{\rho_t/E_t}$ of simply supported FGM nanobeams with the following geometric and material properties: $E_t = 70\,\text{GPa}$, $\rho_t = 2702\,\text{kg/m}^3$, $E_b = 380\,\text{GPa}$, $\rho_b = 3960\,\text{kg/m}^3$, $v_t = v_b = 0.3$ and various nonlocal parameters $\mu^* = (e_0 a/h)^2$, volume fraction indexes and ratios L/h (Aria and Friswell, 2019). As can be seen in Table 1, the calculated results which used the DSM with 1 element are in a very accurate agreement with the results published by Aria and Friswell (2019) who used the FEM with 26 elements. The accurate agreements are received for other boundary conditions such as fixed-pinned, fixed-fixed and fixed-free.

The second comparison is made for nondimensional frequencies $\lambda_i = \omega_i L^2\sqrt{\rho_t A/E_t I}$, $i = 1, 2, 3$ of a portal frame consisting of three beams AB, BC and CD as shown in Fig. 3 (Banerjee and Ananthapuvirajah, 2018). The supports at both points A and D can be either simply supported (Fig. 3a) or clamped (Fig. 3b). All three members of the portal frame are assumed to have the same rectangular cross-section and length of 1 m. The width and height of the cross-section are 0.04 m and 0.02 m, respectively. Numerical computation is accomplished in the three following scenarios:

Table 1. Comparison of the nondimensional fundamental frequencies of FGM nanobeams with various nonlocal parameters, volume fraction indexes and ratios L/h

μ^*	$\kappa = 0.1$		$\kappa = 0.5$		$\kappa = 1$		$\kappa = 2$		$\kappa = 5$	
	$\mathcal{A}$	Present	$\mathcal{A}$	Present	$\mathcal{A}$	Present	$\mathcal{A}$	Present	$\mathcal{A}$	Present
$L/h = 20$										
0	3.3289	3.3289	3.9361	3.9361	4.2051	4.2051	4.4662	4.4662	4.8100	4.8100
1	3.2885	3.2885	3.8884	3.8884	4.1541	4.1541	4.4121	4.4121	4.7518	4.7518
2	3.2496	3.2496	3.8424	3.8424	4.1050	4.1050	4.3599	4.3599	4.6956	4.6956
3	3.2121	3.2121	3.7980	3.7980	4.0576	4.0576	4.3095	4.3095	4.6413	4.6413
4	3.1758	3.1758	3.7551	3.7551	4.0117	4.0117	4.2609	4.2609	4.5889	4.5889
5	3.1408	3.1408	3.7137	3.7137	3.9674	3.9674	4.2138	4.2138	4.5382	4.5382
$L/h = 100$										
0	3.3427	3.3427	3.9512	3.9512	4.2203	4.2203	4.4819	4.4819	4.8272	4.8272
1	3.3411	3.3411	3.9493	3.9493	4.2183	4.2183	4.4797	4.4797	4.8248	4.8248
2	3.3395	3.3395	3.9473	3.9473	4.2162	4.2162	4.4775	4.4775	4.8224	4.8224
3	3.3378	3.3378	3.9454	3.9454	4.2141	4.2141	4.4753	4.4753	4.8200	4.8200
4	3.3362	3.3362	3.9434	3.9434	4.2120	4.2120	4.4731	4.4731	4.8177	4.8177
5	3.3345	3.3345	3.9415	3.9415	4.2100	4.2100	4.4709	4.4709	4.8153	4.8153

$\mathcal{A}$ – Aria and Friswell (2019)

(1) AB and CD are made of an isotropic material, BC is made of an FGM,
(2) AB and CD are made of an FGM, BC is made of a isotropic material,
(3) AB, BC and CD are all made of FGMs.

The isotropic material considered herein is steel with Young's modulus 200 GPa and density 7500 kg/m^3. The FGM is composed of steel on the bottom and ceramic with Young's modulus 380 GPa and density 3960 kg/m^3 on the top.

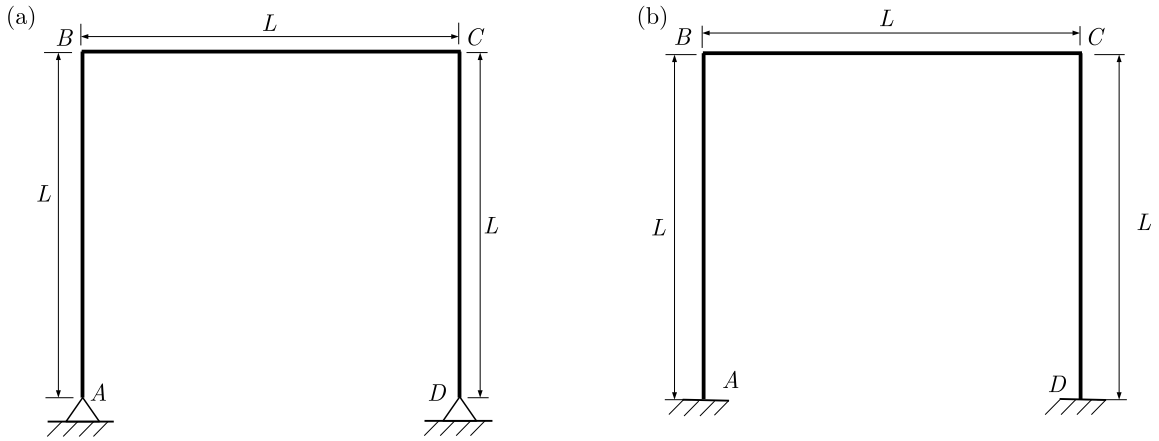

Fig. 3. A portal FGM frame

The first three nondimensional frequencies have been computed by the procedure proposed above and compared to that obtained by Banerjee and Ananthapuvirajah (2018) in the simply supported case at A and D and different values κ (Table 2). Obviously, the discrepancy between the results does not exceed 1.8%. The comparison of the calculated data and published results proves the reliability of the proposed nonlocal dynamic stiffness model.

Table 2. Comparison of the frequency parameter computed in the present study with that given in (Banerjee and Ananthapuvirajah, 2018) for the portal frame

λ	$\kappa = 0.5$		$\kappa = 1$		$\kappa = 5$	
	Present	$\mathcal{A}$	Present	$\mathcal{A}$	Present	$\mathcal{A}$
AB, CD – isotropic; BC – FGM						
λ_1	1.7031	1.6940	1.6424	1.6400	1.5389	1.5410
λ_2	11.1714	11.0830	10.8728	10.8480	10.3528	10.3750
λ_3	16.4054	16.2820	16.0141	15.9610	15.3747	15.3940
AB, CD – FGM; BC – isotropic						
λ_1	1.8361	1.8310	1.7446	1.7520	1.6004	1.6100
λ_2	12.6414	12.6170	11.9589	12.0250	10.8447	10.9210
λ_3	20.2246	20.3010	18.7312	18.9170	16.5509	16.6940
AB, CD, BC – FGM						
λ_1	2.1912	2.2110	1.9802	2.0150	1.6876	1.7080
λ_2	14.7740	14.9060	13.3635	13.5830	11.3785	11.5180
λ_3	22.2309	22.4340	20.1084	20.4380	17.1213	17.3340

$\mathcal{A}$ – Banerjee and Ananthapuvirajah (2018)

3.2. Free vibration of a stepped framed structure

To study the influence of stepped locations, volume fraction index, nonlocal parameter and different boundary conditions on the first three nondimensional frequencies of the nanostructures from this Subsection, the FGM stepped framed structure with geometric and material parameters as follows: $L = 10\,\text{nm}$, $b = h = 1\,\text{nm}$, $E_t = 70\,\text{GPa}$, $\rho_t = 2700\,\text{kg/m}^3$, $E_b = 393\,\text{GPa}$, $\rho_b = 3960\,\text{kg/m}^3$, $v_t = v_b = 0.3$ will be discussed (Fig. 3). The calculated results for the first three nondimensional frequencies $\lambda_i = \omega_i L^2\sqrt{\rho_t A/E_t I}$, $i = 1, 2, 3$ include boundary conditions: 1) simply supported at both ends (S-S); 2) clamped at A and free at D (C-F); 3) clamped at both ends (C-C); and 4) clamped at A and simply supported at D (C-S), respectively. The stepped height locations with $h_1/h = 0.8$ move from A to D, where $L_1/L = 0$ corresponds to $h_1 = 0.8h$ on the whole beam, $L_1/L = 1$ corresponds to $h_1 = h$ along the beam (Fig. 4).

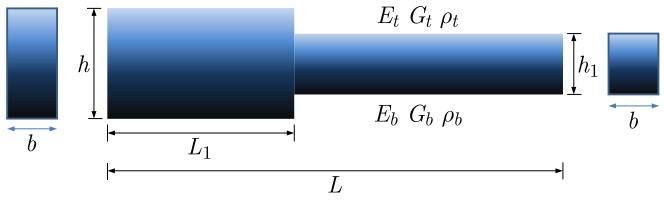

Fig. 4. A FGM nanobeam with stepped height

Figures 5 and 6 show the changes of the first three nondimensional frequencies of stepped FGM framed structures with different stepped locations, nonlocal parameter $\mu^* = (e_0 a/h)^2$, volume fraction indexes and boundary conditions: S-S (Figs. 5a-c), C-F (Figs. 5d-f), C-C (Figs. 6a-c), C-S (Figs. 6d-f). Observing the graphs given in Figs. 5a-l allows one to make the following remarks:

- There exist positions or structural elements on FGM structures at which stepped locations appear and make a distinct effect on certain nondimensional frequencies, especially the fundamental frequency. Such positions are called here critical points for a given frequency. Knowing the critical points, one can select stepped locations or structural elements of the nanostructure in order to achieve the maximum or minimum values for the given frequency (Figs. 5a,d,e,f and Figs. 6a,d). For example, as shown in Fig. 5a, the fundamental frequency

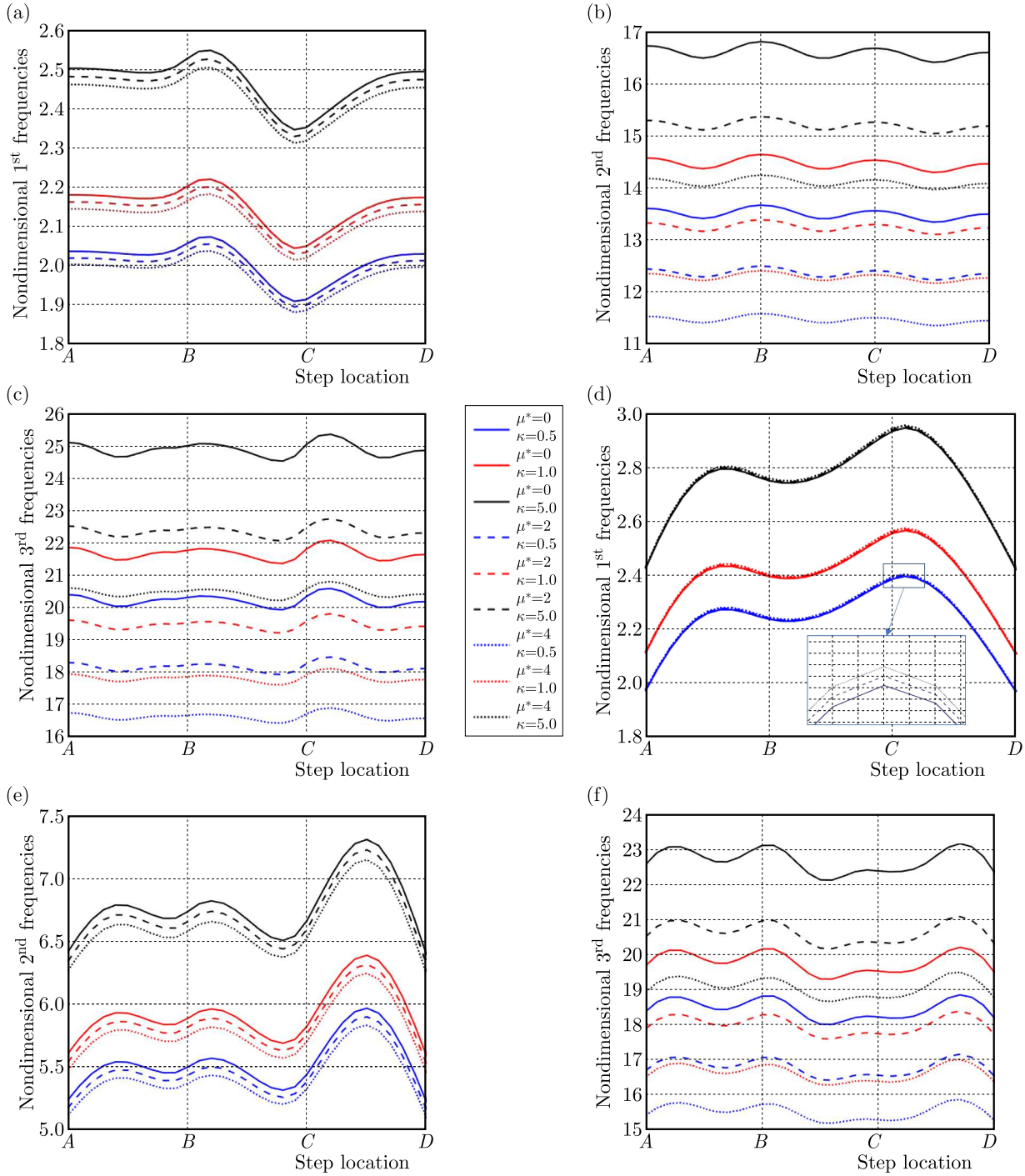

Fig. 5. Changes of the first three nondimensional frequencies of stepped FGM framed structures with different stepped locations, nonlocal parameter, volume fraction indexes and boundary conditions: (a)-(c) *S*-*S*, (d)-(f) *C*-*F*

achieves the maximum and minimum values corresponding to the stepped locations at $0.3L$ and at $0.9L$ of the beam BC. The stepped locations on the beam BC make distinct variations to the fundamental frequency of structures with the boundary conditions *S*-*S*.

- The changes of nondimensional fundamental frequencies of the stepped nanostructures caused by the volume fraction indexes are more distinct than those caused by nonlocal parameters (Figs. 5a,d and Figs. 6a,d). The gaps between every two consecutive graphs follow the same increasing trend of the volume fraction index.

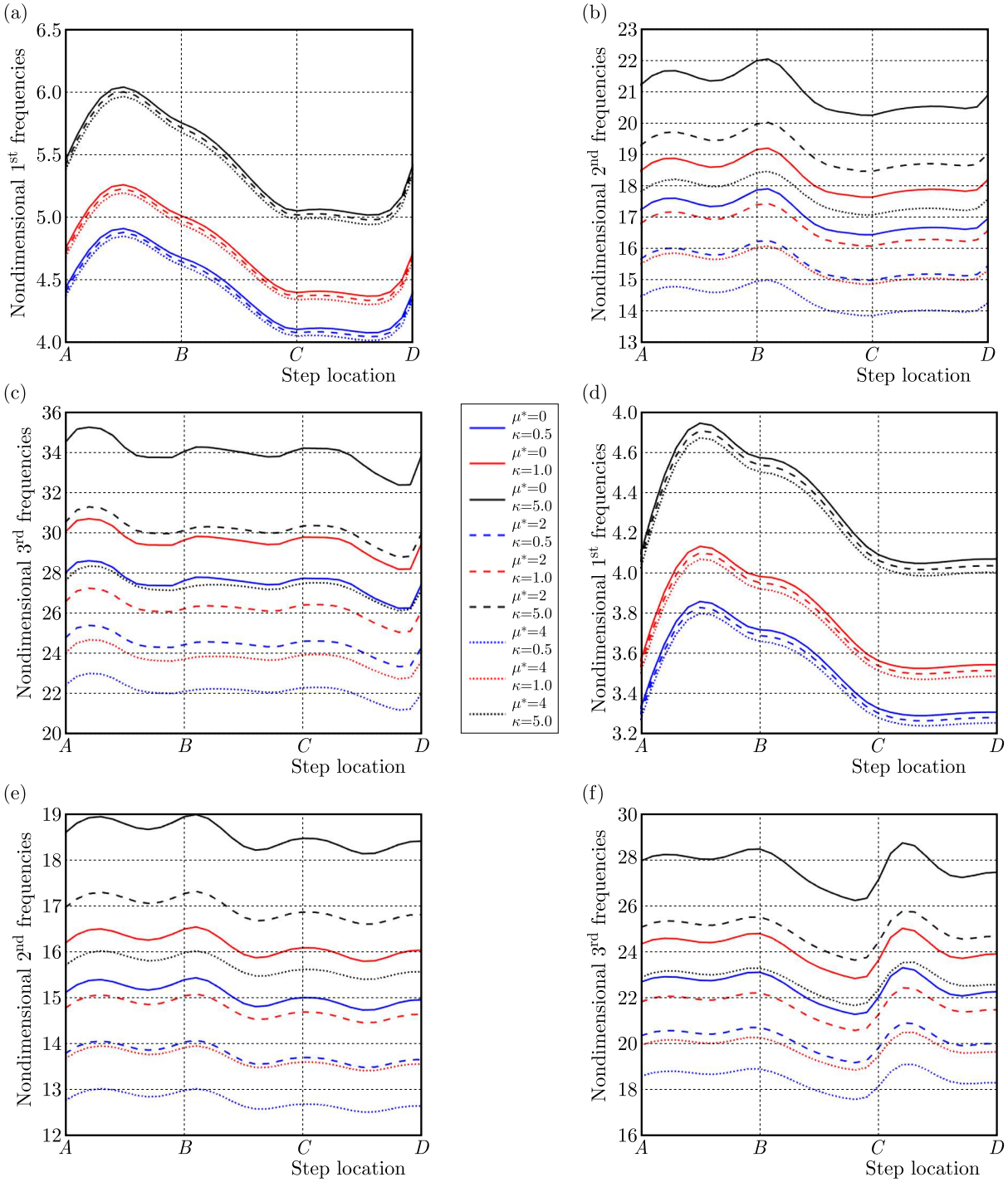

Fig. 6. Changes of the first three nondimensional frequencies of stepped FGM framed structures with different stepped locations, nonlocal parameter, volume fraction indexes and boundary conditions: (a)-(c) *C-C*, (d)-(f) *C-S*

- When the nonlocal parameter increases, the nondimensional fundamental frequencies in *S-S*, *C-C* and *C-S* boundary conditions decrease while the nondimensional fundamental frequency for the cantilever beam increases (Fig. 5d). This nonlocal paradox of FGM nanostructures was also mentioned in (Li and Wang, 2009; Eltaher *et al.*, 2013b; Ghavanloo *et al.*, 2019; Taima *et al.*, 2020) when considering vibration of Euler-Bernoulli and Timoshenko homogeneous nanobeams.

- The nondimensional frequencies achieved by the C-C boundary condition are higher than C-S, S-S and C-F in most cases.

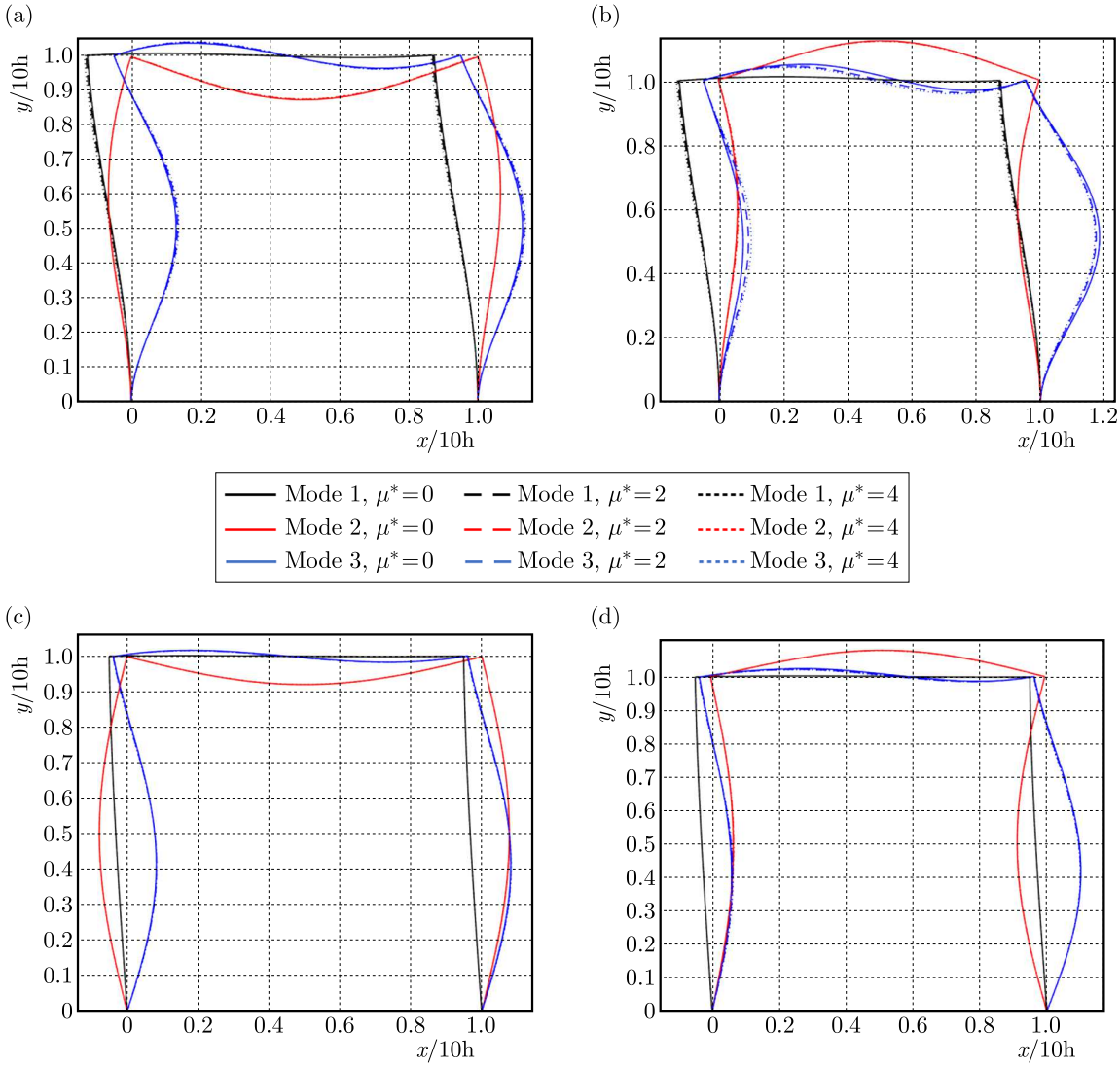

Fig. 7. The first three mode shapes of the FGM framed structure with different stepped locations, nonlocal parameter and boundary conditions: (a) C-C with constant height, (b) C-C with the stepped location at $0.3L$ on the beam BC, (c) S-S with constant height, (d) S-S with the stepped location at $0.3L$ on the beam BC. For all plots, the volume fraction index κ is equal to 5

Figure 7 shows the first three mode shapes of the FGM framed structure with different stepped locations, nonlocal parameter and the boundary conditions C-C (Figs. 7a,b) and S-S (Figs. 7c,d). Figure 8 shows the first three mode shapes of the FGM framed structure with different stepped locations, volume fraction indexes and the boundary conditions C-C (Figs. 8a,b) and S-S (Figs. 8c-d). Observing the graphs given in Figs. 7 and 8 allows one to make the following remarks:

- Contrary to the changes of nondimensional frequencies, the changes of mode shapes of the stepped nanostructures caused by nonlocal parameters are more distinct than those caused by the volume fraction indexes. Moreover, the changes of mode shapes of the stepped nanostructures are more distinct than those of the non-stepped nanostructures.

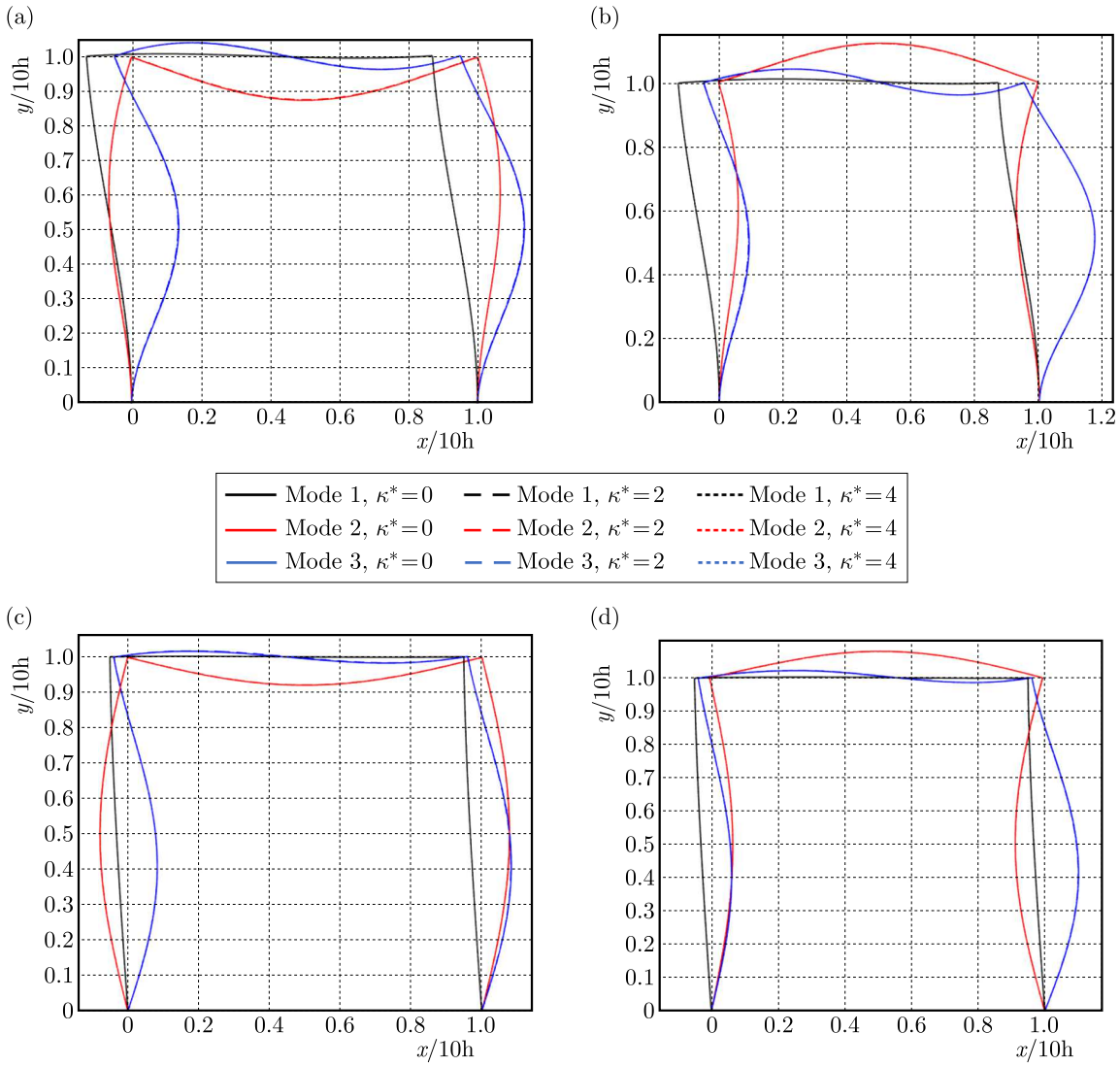

Fig. 8. The first three mode shapes of the FGM framed structure with different stepped locations, volume fraction indexes and boundary conditions: (a) C-C with constant height, (b) C-C with the stepped location at $0.3L$ on the beam BC, (c) S-S with constant height, (d) S-S with the stepped location at $0.3L$ on the beam BC. For all plots, the nonlocal parameter μ^* is equal to 2

- The changes of the unsymmetric mode shapes (mode 1 and 3) of the stepped nanostructures caused by nonlocal parameters are clearer than the changes of the symmetric mode shape (mode 2).
- When the nonlocal parameter increases, the mode shapes of nanostructures for S-S boundary conditions are the same as the corresponding mode shapes for local Timoshenko beams (Figs. 7c,d and Figs. 8c,d). This nonlocal paradox of FGM nanostructures was also mentioned in (Wang *et al.*, 2007; Li and Wang, 2009) when considering vibration of Timoshenko homogeneous nanobeams.

4. Conclusion

In the present paper, a nonlocal dynamic stiffness model is proposed to investigate free vibration of FGM stepped nanostructures based on the Nonlocal Elasticity Theory (NET) and Timoshenko beam theory. The dynamic stiffness model fulfilled the gap of the finite element method by using

frequency-dependent shape functions that are found as an exact solution of the vibration problem in the frequency domain and could capture all necessary high frequencies and mode shapes of interest. Comparison with the published results of other authors shows the reliability of the proposed nonlocal dynamic stiffness model.

On that basis, the influence of nonlocal parameters, materials, geometric parameters and boundary conditions on the vibration frequencies and mode shapes of FGM stepped nanostructures is investigated. The results obtained from this paper show that there exist critical points, stepped locations at which the effect on a given frequency is distinct. The nondimensional fundamental frequency of stepped FGM structures is most sensitive to the stepped locations and boundary conditions. Also, the changes of the first three frequencies of the stepped nanostructures caused by the volume fraction index are more distinct than those caused by nonlocal parameters. The gap between every two consecutive graphs of the changes of nondimensional frequencies of FGM stepped structures with different stepped locations, nonlocal parameter and boundary conditions increase with the decreasing nonlocal parameter and increasing volume fraction index. Contrary to the changes of nondimensional frequencies, the changes of mode shapes of the stepped nanostructures caused by nonlocal parameters are more distinct than those caused by the volume fraction indexes. And the changes of mode shapes of the stepped nanostructures are more distinct than those of the non-stepped nanostructures. The present research also shows two cases of the "nonlocal paradox of FGM nanostructures":

- The first frequency of nanostructures with *C-F* boundary conditions increases as the other frequencies decrease;
- The mode shapes of nanostructures with *S-S* boundary conditions are the same as the corresponding mode shapes for local Timoshenko beams.

All the mentioned notices are a useful indication for vibration analysis of FGM nanostructures. The study can be applied to more complex stepped nanostructures.

Acknowledgement

This research was funded by National University of Civil Engineering under grant number 35-2020/KHXD-T.

References

1. Aria A., Friswell M., 2019, A nonlocal finite element model for buckling and vibration of functionally graded nanobeams, *Composites Part B: Engineering*, **166**, 233-246
2. Banerjee J., Ananthapuvirajah A., 2018, Free vibration of functionally graded beams and frameworks using the dynamic stiffness method, *Journal of Sound and Vibration*, **422**, 34-47
3. Chakraverty S., Behera L., 2015, Free vibration of non-uniform nanobeams using Rayleigh--Ritz method, *Physica E: Low-Dimensional Systems and Nanostructures*, **67**, 38-46
4. Ebrahimi F., Nasirzadeh P., 2015, A nonlocal Timoshenko beam theory for vibration analysis of thick nanobeams using differential transform method, *Journal of Theoretical and Applied Mechanics*, **53**, 4, 1041-1052
5. Ebrahimi F., Salari E., 2015, A semi-analytical method for vibrational and buckling analysis of functionally graded nanobeams considering the physical neutral axis position, *CMES – Computer Modeling in Engineering and Sciences*, **105**, 2, 151-181
6. Eltaher M., Alshorbagy A., Mahmoud F., 2013a, Determination of neutral axis position and its effect on natural frequencies of functionally graded macro/nanobeams, *Composite Structures*, **99**, 193-201
7. Eltaher M., Alshorbagy A.E., Mahmoud F., 2013b, Vibration analysis of Euler-Bernoulli nanobeams by using finite element method, *Applied Mathematical Modelling*, **37**, 7, 4787-4797

8. Eringen A.C., 2002, *Nonlocal Continuum Field Theories*, Springer Science & Business Media

9. Ghavanloo E., Rafii-Tabar H., Fazelzadeh S.A., 2019, *Computational Continuum Mechanics of Nanoscopic Structures*, Springer

10. Jena S.K., Chakraverty S., 2018, Free vibration analysis of variable cross-section single layered graphene nano-ribbons (SLGNRs) using differential quadrature method, *Frontiers in Built Environment*, **4**, 63

11. Karličić D., Murmu T., Adhikari S., McCarthy M., 2015, *Non-Local Structural Mechanics*, John Wiley & Sons

12. Li X.-F., Wang B.-L., 2009, Vibrational modes of Timoshenko beams at small scales, *Applied Physics Letters*, **94**, 10, 101903

13. Lien T.V., Ngo D.T., Nguyen K.T., 2019, Free and forced vibration analysis of multiple cracked FGM multi span continuous beams using dynamic stiffness method, *Latin American Journal of Solids and Structures*, **16**, 2

14. Malikan M., Wiczenbach T., Eremeyev V.A., 2021, Thermal buckling of functionally graded piezomagnetic micro- and nanobeams presenting the flexomagnetic effect, *Continuum Mechanics and Thermodynamics*, 1-16

15. Mechab I., El Meiche N., Bernard F., 2016, Free vibration analysis of higher-order shear elasticity nanocomposite beams with consideration of nonlocal elasticity and Poisson effect, *Journal of Nanomechanics and Micromechanics*, **6**, 3, 04016006

16. Narendar S., Gopalakrishnan S., 2011, Spectral finite element formulation for nanorods via nonlocal continuum mechanics, *Journal of Applied Mechanics*, **78**, 6, 061018

17. Rahmani O., Pedram O., 2014, Analysis and modeling the size effect on vibration of functionally graded nanobeams based on nonlocal Timoshenko beam theory, *International Journal of Engineering Science*, **77**, 55-70

18. Reddy J., 2007, Nonlocal theories for bending, buckling and vibration of beams, *International Journal of Engineering Science*, **45**, 2-8, 288-307

19. Şimşek M., Yurtcu H., 2013, Analytical solutions for bending and buckling of functionally graded nanobeams based on the nonlocal Timoshenko beam theory, *Composite Structures*, **97**, 378-386

20. Su H., Banerjee J., 2015, Development of dynamic stiffness method for free vibration of functionally graded Timoshenko beams, *Computers and Structures*, **147**, 107-116

21. Taima M.S., El-Sayed T.A., Farghaly S.H., 2020, Free vibration analysis of multistepped nonlocal Bernoulli-Euler beams using dynamic stiffness matrix method, *Journal of Vibration and Control*, **27**, 7-8, 774-789

22. Trinh L.C., Vo T.P., Thai H.-T., Nguen T.-K., 2018, Size-dependent vibration of bi-directional functionally graded microbeams with arbitrary boundary conditions, *Composites Part B: Engineering*, **134**, 225-245

23. Usharani R., Uma G., Umapathy M., Choi S.-B., 2018, A novel piezoelectric energy harvester using a multi-stepped beam with rectangular cavities, *Applied Sciences*, **8**, 11, 2091

24. Uymaz B., 2013, Forced vibration analysis of functionally graded beams using nonlocal elasticity, *Composite Structures*, **105**, 227-239

25. Wang C., Zhang Y., He X., 2007, Vibration of nonlocal Timoshenko beams, *Nanotechnology*, **18**, 10, 105401

Manuscript received October 6, 2021; accepted for print March 25, 2022